

Structure-Related Optical Fingerprints in the Absorption Spectra of Colloidal Quantum Dots: Random Alloy vs. Core/Shell Systems

Daniel Mourad^{1, a)}

Institute for Theoretical Physics, University of Bremen, Otto-Hahn-Allee 1, 28359 Bremen, Germany

(Dated: November 10, 2018)

We argue that the experimentally easily accessible optical absorption spectrum can often be used to distinguish between a random alloy phase and a stoichiometrically equivalent core/shell realization of ensembles of monodisperse colloidal semiconductor quantum dots without the need for more advanced structural characterization tools. Our proof-of-concept is performed by conceptually straightforward exact-disorder tight-binding calculations. The underlying stochastic tight-binding scheme only parametrizes bulk band structure properties and does not employ additional free parameters to calculate the optical absorption spectrum, which is an easily accessible experimental property. The method is applied to selected realizations of type-I Cd(Se,S) and type-II (Zn,Cd)(Se,S) alloyed quantum dots with an underlying zincblende crystal structure and the corresponding core/shell counterparts.

PACS numbers: 73.22.Dj, 78.67.Hc, 71.35.Cc, 71.23.-k

I. INTRODUCTION

It is well established that the optoelectronic properties of colloidal semiconductor quantum dots (QDs, also known as semiconductor nanocrystals) can be tuned by means of alloying, i.e., the use of solid solutions of a multitude of compounds. These alloyed systems exhibit a usually complicated and nonlinear combination of the material properties of their constituents. As an example, it is possible to vary the stoichiometry of few-nanometer sized (Cd,Zn)(Se,S) alloyed QDs to shift the optical gap over the visible spectral range.¹ To make the distinction between a randomly alloyed QD and the corresponding stoichiometrically equivalent core/shell counterpart is difficult, especially for small diameters of the nanocrystals. It has been shown that rather sophisticated characterization tools like Raman spectroscopy can be used to confirm the presence of solid-solution nanocrystals,² as well as partial alloying.³ However, an identification based on an optical measurement (such as the UV-vis absorption spectrum) would clearly be advantageous due to the simplicity of the approach. Also, it would circumvent the need for a modification and re-interpretation of the already rather involved bulk Raman selection rules for nanosized systems with complicated boundary conditions.

In a recent publication,⁴ we have shown for the example of Cd(Se,S) that alloyed semiconductor QDs show fingerprints in their absorption spectrum that can be traced back to the inherent breakdown of point group symmetries in random systems, which subsequently leads to a lifting of selection rules. We further pointed out that these features can be reproduced and analyzed by means of conceptionally simple stochastic tight-binding (TB)

simulations that emulate the disorder degree of freedom on finite ensembles. Moreover, we concluded that a feasible analysis is already possible on a single-particle level including the light-matter coupling in the dipole approximation.

In the present work, we will explore whether similar calculations can be used in general to unambiguously identify randomly alloyed QDs—as opposed to their stoichiometrically identical but phase-separated core/shell counterparts—by their linear absorption spectrum. The method is applied to type-I Cd(Se,S) and type-II (Zn,Cd)(Se,S) alloyed quantum dots; the latter will be compared to core/shell realizations with a CdS core and a ZnSe shell and vice versa. We restrict our discussion to QDs with a diameter of $d \approx 3$ nm, which corresponds to 5 conventional lattice constants of the zincblende crystal structure for the materials under consideration.

II. THEORY

The underlying theoretical framework of the here employed stochastic TB approach has already been explained in detail in Ref. 4 and the references therein. Therefore, we will here only give a brief outline of the most relevant features and will put more emphasis on eventual modifications and simplifications which are required to cope with the numerical complexity of the task at hand.

A. Tight-Binding Model

The empirical bulk TB approach employed in this paper is based on a parametrization of eight Wannier-like orbitals $|\mathbf{R}\alpha\rangle \otimes |\sigma\rangle$, where $\alpha \in \{s, p_x, p_y, p_z\}$, $\sigma = \{\uparrow, \downarrow\}$ and \mathbf{R} labels the underlying fcc lattice sites

^{a)}Electronic mail: dmourad@itp.uni-bremen.de

of the zincblende structure.⁵ In this approach, non-vanishing tight-binding matrix elements (TBME) of the bulk Hamiltonian $\langle \mathbf{R}\alpha | H_{\text{bulk}} | \mathbf{R}'\alpha' \rangle$ up to the second nearest neighbor shell are used to accurately reproduce the dressed electronic band structure of one conduction and three valence bands per spin projection throughout the whole Brillouin zone in accordance with input from experiment or *ab initio* quasiparticle calculations. The corresponding input parameters for CdS, CdSe and ZnSe as well as their original sources can be found in Table I.

B. Simulation of randomly alloyed and core/shell QDs

For the randomly alloyed A_xB_{1-x} QDs, the site-diagonal TBMEs of the pure constituents are determined stochastically, where the probability of using an A or B TBME is given by the respective compositions x and $1 - x$. To cover relevant portions of the visible spectrum, 100 electron and 1000 hole energies $e_{i,n}, h_{i,n}$ and TB wave functions $\psi_{i,n}^{e/h}$ are obtained by means of exact diagonalization, where n labels the different microstates (mimicking the individual QD in a large sample). The term “microstate” is here used as common in statistical physics and designates a specific microscopically identifiable configuration of an alloyed QD that is characterized by the exact spatial distribution of the lattice sites with either A or B material. This procedure is then repeated $N = 25$ times for each stoichiometric ratio, which turned out to be a suitable compromise between the convergence accuracy and the numerical effort. The energy scales of A and B are aligned via the bulk valence band offset value ΔE_{vb} . Intersite matrix elements between A and B are approximated by their arithmetic average. To emulate the spatial confinement of the approximately spherical QDs, we set the hopping probability at the surface to zero. This corresponds to a perfect surface passivation. Strain and relaxation effects are not included in our TB scheme. This can heuristically be justified by the rather small lattice mismatch for the material combinations under consideration ($< 3\%$ for CdS/ZnSe, $\approx 4\%$ for CdS/CdSe). Furthermore, the proper inclusion of bond-length and bond-angle variations into the bulk-parametrized TB calculations is conceptually difficult for the surface/volume ratios considered here. We would have to model the impact of different boundary conditions, e.g., solid-liquid, solid-solid or solid-air interfaces which has lead to not only ambiguous but even diametrically opposed results for the nature of the strain field in recent studies on II-VI core/shell systems. A striking example is given by the conflicting conclusions by [Tschirner et al.](#) for CdSe/CdS QDs in Ref. 3 (prediction of tensile strain in shell) and [Han and Bester](#) in Ref. 11 (prediction of compressive strain in shell). These studies also reveal that the nature of the strain field is heavily dependent on the exact modeling of the boundary conditions at the QD surface. Therefore, our pragmatic decision to use hard-wall boundary conditions and neglect strain effects

altogether prevents the afore cited unresolved ambiguities, but will definitely have an impact on the quantitative accuracy of our results, which cannot be judged rigorously within our present study. On the plus side, the computational effort is diminished, as the strain field and the subsequent corrections to our TBMEs would additionally have to be computed for each single realization of the QDs in the ensemble, alongside a careful testing and fitting procedure for the distance scaling law of the TBME.

C. Optical properties

The transition probability for converting a photon into an electron-hole pair is obtained on the footing of Fermi's golden rule,

$$I(\omega) = \frac{2\pi}{\hbar} \frac{1}{N} \sum_{n=1}^N \sum_{i,f} |\langle \Psi_n^f | H_D | \Psi_n^i \rangle|^2 \delta(E_n^i - E_n^f - \hbar\omega), \quad (1)$$

where n labels the initial/final states $|\Psi_n^{i/f}\rangle$ of the microscopically distinct configurations with energies $E_n^{i/f}$, \hbar is the reduced Planck constant, ω the absorption frequency and H_D is the light-matter coupling Hamiltonian in the long-wavelength approximation. In other words, for each fixed stoichiometric ratio we first calculate separate $I(\omega)$ curves for each of the $N = 25$ different random QDs and then superpose them in an attempt to emulate the spectrum of the macroscopic ensemble. This also encompasses the model assumption that the individual QDs in our *in silico* computational “sample” do not interact explicitly by any means.

As we use hard-wall boundary conditions on finite supercells¹² and a strictly local TB Hamiltonian,¹³ the matrix elements (MEs) of H_D can be unambiguously calculated from the MEs of the position operator between the electron and hole states $|\psi_i^{e/h}\rangle$ which constitute the $|\Psi_n^{i/f}\rangle$,

$$\mathbf{d}_{ij}^{eh} = e_0 \langle \psi_i^e | \mathbf{r} | \psi_j^h \rangle, \quad (2)$$

where e_0 is the electron charge, \mathbf{r} is approximated by the Bravais lattice operator $\mathbf{r} \approx \sum_{\mathbf{R}\alpha} |\mathbf{R}\alpha\rangle \mathbf{R} \langle \mathbf{R}\alpha|$ ¹⁴ and the $|\psi_i^{e/h}\rangle$ are constituted by their expansion coefficients in the TB basis orbitals. This diagonal form of the position operator is gauge invariant, see, e.g., Ref. 15. Albeit the short-range contributions from the wave functions do not enter explicitly, it should be stressed that our approach is on a higher level of sophistication than the usual multi-band cell-envelope factorization¹² in the envelope function approximation. In our model, the potential landscape of the alloy is resolved in lattice resolution and the orbital character of the underlying orbitals is also probed.

Table I. Material parameters that were used to fit the tight-binding matrix elements, including the references. CB and VB stand for conduction and valence band, respectively.

| | | | CdSe | Ref. | CdS | Ref. | ZnSe | Ref. |
|-----------------|-------------------------------|-----------|-------|------|-------|------|-------|------|
| E_g | bulk band gap | (eV) | 1.68 | 6 | 2.46 | 6 | 2.68 | 7 |
| m_c | CB effective mass | $(m_0)^*$ | 0.12 | 8 | 0.14 | 6 | 0.147 | 8 |
| γ_1 | VB Luttinger parameters | | 3.33 | 8 | 4.11 | 6 | 2.45 | 9 |
| γ_2 | | | 1.11 | 8 | 0.77 | 6 | 0.61 | 9 |
| γ_3 | | | 1.45 | 8 | 1.53 | 6 | 1.11 | 9 |
| Δ_{so} | spin-orbit splitting | (eV) | 0.41 | 8 | 0.078 | 6 | 0.43 | 8 |
| X_1^c | CB X point energy | (eV) | 2.94 | 7 | 5.24 | 6 | 4.41 | 7 |
| X_5^v | VB X point energies | (eV) | -1.98 | 7 | -1.9 | 6 | -2.08 | 7 |
| X_3^v | | (eV) | -4.28 | 7 | -4.8 | 6 | -5.03 | 7 |
| ΔE_{vb} | VB offset | (eV) | 0.4 | 10 | 0 | 10 | 0.35 | 10 |
| a | conventional lattice constant | (Å) | 6.078 | 8 | 5.825 | 6 | 5.668 | 8 |

* Free electron rest mass.

D. Coulomb effects and dielectric confinement

Surface polarization effects due to the dielectric mismatch at the QD boundaries are currently neglected; the $|\Psi_n^{i/f}\rangle$ can then in principle be obtained in a basis of Slater determinants that are constructed from the $|\psi_i^{e/h}\rangle$ after the corresponding Coulomb interaction MEs have been computed at a desired level of sophistication (see, e.g., Refs. 16–18 for a detailed description of a TB-based approach). This procedure (which represents a simplified TB treatment of the Bethe-Salpeter equation for excitons¹⁹) was feasible in Ref. 4, where the necessary number of basis states was significantly lower due to the focus on a small energy window. Also, the influence of the additional disorder degree of freedom on the Coulomb ME had yet to be examined in detail in this paper. However, for a cardinality of the basis as employed in the present work, such calculations are still not viable even with the help of modern supercomputers, as it would involve the calculation of $\sim 10^{11}$ Coulomb MEs per composition.

Consistent with the findings of Delerue *et al.* in Ref. 20, we will instead make use of a cancellation effect and calculate the excitonic absorption spectrum directly in the single-particle basis (i.e., dressed by bulk interactions) without the explicit incorporation of Coulomb MEs. Their work concentrated on the nature of the fundamental gap of Si nanocrystals, where they expressed the excitonic gap ϵ_g^{exc} (the energetically lowest transition energy) as:

$$\epsilon_g^{\text{exc}} = \epsilon_g^{\text{qp}} - E^{\text{coul}} = \epsilon_g^0 + \delta\Sigma - E^{\text{coul}} \quad (3)$$

Here, the quantity ϵ_g^{qp} is the quasiparticle gap and E^{coul} is the attractive interaction between a quasi-electron and a quasi-hole. $\delta\Sigma := \epsilon_g^{\text{qp}} - \epsilon_g^0$ is the self-energy correction to the “independent particle gap” ϵ_g^0 . The latter is basically defined by the partitioning of Eq. (3) and can,

e.g., be obtained from an *ab initio* LDA calculation as the HOMO-LUMO difference. Within an empirical TB model, augmented by *GW* and Bethe-Salpeter calculations, Delerue *et al.* then showed that the QD-specific deviation of the self energy from its bulk value $\delta\Sigma - \delta\Sigma_{\text{bulk}}$ actually cancels with E^{coul} for a large range of QD diameters $d \geq 1.5$ nm. Furthermore, they showed that the largest contribution to $\delta\Sigma - \delta\Sigma_{\text{bulk}}$ can be interpreted in terms of classical electrostatics as a surface-induced polarization term $\Sigma_{\text{pol}} \approx \delta\Sigma - \delta\Sigma_{\text{bulk}}$ which is not included in a standard non self-consistent scheme like our present TB model. As a consequence of the cancelling effect, one is left with

$$\epsilon_g^{\text{exc}} \approx \epsilon_g^0 + \delta\Sigma_{\text{bulk}} = e_1 - h_1, \quad (4)$$

where e_1/h_1 are the lowest/highest TB electron/hole energies of the QD system. The last equation is valid because $\delta\Sigma_{\text{bulk}} = 0$ holds in an empirical TB approach, where the dressed single-particle gap values will effectively contain all bulk-related interactions by means of the fitting procedure. Also, they found that the results were transferable to other materials (Ge and C in their study) and do not change upon the exact treatment of the surface passivation. It should, however, be pointed out that their results were obtained for QDs that were embedded in media with low polarizability (e.g. vacuum or air), where the dielectric constant ϵ_{out} of the medium is close to unity, while the Si QDs had a several times larger average polarizability, reflected in a corresponding value ϵ_{in} .

E. Generality of approach

In Appendix A, we elaborate why we also consider this approach sufficiently accurate for the present systems under consideration for a discussion of the optical spectrum

as presented in this paper. Nevertheless, it should be emphasized that the main results of the present work are of a *qualitative* nature and do *not* rely on the full transferability of the canceling effect reported by Delerue *et al.* to our II-VI systems. We also stress again at this point that our calculations do not use microscopically realistic surface boundary conditions and neglect strain-induced effects, which prevents model-intrinsic ambiguities but hampers quantitatively accurate predictions. However, as long as the weaker assumptions listed below are valid (as in detail discussed in the Appendix), we are left with $\delta\Sigma - E^{\text{coul}} \approx \text{const.}$, resulting only in a phase independent constant shift of *both* the core/shell and random alloy spectra:

- The macroscopic dielectric response of the core/shell and randomly alloyed QDs can be described by a *common* $\epsilon_{\text{in}}^{-1}$. Consequently, the surface-induced polarization Σ_{pol} does not depend on the phase of the QD, as it is a function of $\epsilon_{\text{out}}^{-1} - \epsilon_{\text{in}}^{-1}$.^{21,22}
- The variation of electron-hole Coulomb interaction MEs upon phase segregation is small on the eV energy scale that covers the visible range.

Both of these points should actually hold for a broad class of materials: (i) The inverse macroscopic dielectric constants of QDs consisting of different miscible isovalent compound semiconductors are usually very similar for small systems. According to Delerue *et al.*,²³ the reduction of the screening constant in small crystallites can then mainly be attributed to the breaking of the polarizable bonds at the surface. (ii) The Coulomb interaction MEs are dominated by the strong confinement of the charge carrier wave functions. Our previous work^{4,18} has shown that dipole selection rules react sensitively to alloy-induced disorder, while the electron-hole attraction is not overly sensible to such perturbations. This will also apply to small isovalent core/shell QDs with thin shells, as the confinement of the charge carriers is dominated by the large (in our model infinite) discontinuity at the QD boundary and the wave functions leak across the internal interface.

III. RESULTS AND DISCUSSION

A. Choice of material system and stoichiometric ratios

In the following, we will, for reasons of numerical effort as well as for the sake of brevity, confine the discussion to selected realizations with representative stoichiometric ratios. All QDs have a diameter of 5 conventional lattice constants a , which corresponds to $d \approx 3$ nm for the material systems under consideration. Throughout this paper, we will employ a name convention that is derived from the corresponding bulk interface energetics. A sketch of the respective bulk band line-up (using the

Band line-up scheme of bulk input parameters

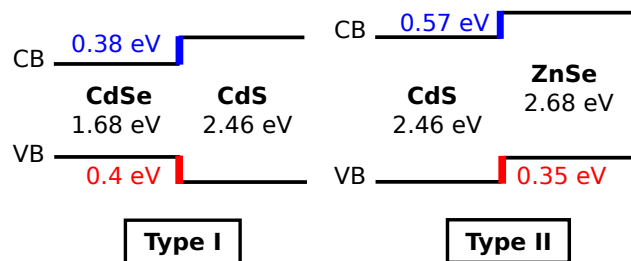


Figure 1. Scheme of the energetic line-up of the *bulk* conduction band (CB) and valence band (VB) edges for the material combinations that are investigated in the present paper, including the band gap values (black), conduction band offsets (blue) and valence band offsets (red).

material parameters from Table I) can be found in Figure 1.

According to Figure 1, the CdSe/CdS core/shell system then represents a type-I lineup, i.e., for large enough systems both the electron and hole states in the vicinity of the fundamental gap are both predominantly localized in the core region. In contrast, the type-II CdS/ZnSe core/shell line-up confines the lowest electron states to the core and the energetically highest hole states to the shell region for large enough cores and shells. These features are reversed in the type-II ZnSe/CdS system. It should be noted that another convention is to denote the line-up characteristics based on the ground state electron and hole wave function localization, which then introduces intermediate classes (e.g., “type-I-1/2” or “quasi type-II” where one of the charges is spread over the QD, while the other is localized to the core or shell, respectively).²⁴ We prefer the more general bulk-related name convention as our calculations expand on a bulk band structure scheme and the carrier overlap naturally enters the absorption spectrum by means of the dipole MEs, Eq. (2). Moreover, any of the randomly alloyed QD systems can anyway only be strictly classified by their pure bulk constituents’ line-up.

The application-relevant type-I and type-II core/shell realizations usually exhibit thicker cores and shells than in the present work (see, e.g., Ref. 25) to enhance their optical properties. Also, these QDs often exhibit more or less significant additional modifications like interfacial alloying or a wurtzite phase.^{25,26} This will not concern us here, as we focus on the distinction between alloyed QDs and their “undesired” segregated core/shell counterparts, rather than on the simulation of tailor-made core/shell QDs.

Type-I QDs. We simulate CdSe_{0.25}S_{0.75} randomly alloyed QDs and their CdSe/CdS core/shell counterpart, which corresponds to a CdSe core diameter of $5a$ coated by a CdS shell of a thickness of $1a$ (hence one layer of CdS

unit cells, i.e., approximately 0.6 nm). Both of these stoichiometrically equivalent QD types are in principle experimentally available²⁷ and relevant for a broad range of applications.^{2,4,25,28–31} Specifically, the alloyed Cd(Se,S) QDs cover the visible spectrum for the size simulated here. Therefore, they also constitute a suitable benchmark system for the predictive power as well as the limitations of our model calculations.

Type-II QDs. Here, we consider two different classes of stoichiometrically equivalent systems: (a) $\text{Cd}_{0.25}\text{Zn}_{0.75}\text{S}_{0.25}\text{Se}_{0.75}$ randomly alloyed QDs and their CdS/ZnSe core/shell counterpart with the same geometry as described above. The former QDs represents a realization of the quarternary (Zn,Cd)(Se,S) alloy, as realized, e.g., in Ref.1, while the latter is a promising candidate for QD lasing.³² (b) $\text{Cd}_{0.75}\text{Zn}_{0.25}\text{S}_{0.75}\text{Se}_{0.25}$ randomly alloyed QDs and their respective ZnSe/CdS core/shell version, which can be used in photovoltaics³³ or as a starting point for electronic tuning upon gradual interface alloying.³⁴

In all calculations, we use a light polarization along the [100] direction without loss of generality. For measurements on a real macroscopic ensemble, where all orientations are present, any directional dependence will cancel out. In our model calculations for alloys on finite ensembles, the statistical averaging over the realizations will approximately have the same effect, whereas in the core/shell systems the linear optical susceptibility is a tensor of rank two, of which the matrix representation has three degenerate eigenvalues in systems with cubic symmetry. Inversion asymmetry and fine structure related effects are beyond the scope of the present work and will not contribute on the scale of energetic resolution that is discussed here.

All calculations use a broadening of the δ -peaks in Eq. 1 that would correspond to a full width at half maximum of ca. 120 meV for a hypothetical isolated excitation peak at energy $e_i - h_j, i, j = \text{const}$. This exact value had already been used for the detailed analysis in Ref. 4. The numerical line broadening will in practice also partially incorporate a multitude of effects beyond the lifetime of the transition, e.g., the finite cardinality of the statistical sample as well as any size and shape fluctuations and uncertainties that could in principle be included explicitly in our model but would significantly enlarge the numerical effort. It should be pointed out that the above mentioned broadening parameter has *not* been varied furtherly to “fine-tune” the individual spectra. Doing so, one could achieve a better agreement with the experimental line shapes. However, we refrain from such an approach, as it would obscure the predictive power and limitations of our stochastic TB scheme. In contrast, we emphasize that no additional free parameters beyond the necessary fitting to bulk electronic properties have been used in our model.

In the following, we will discuss the optical absorption spectra for the type-I system and the type-II systems, respectively. All spectra have been normalized to a com-

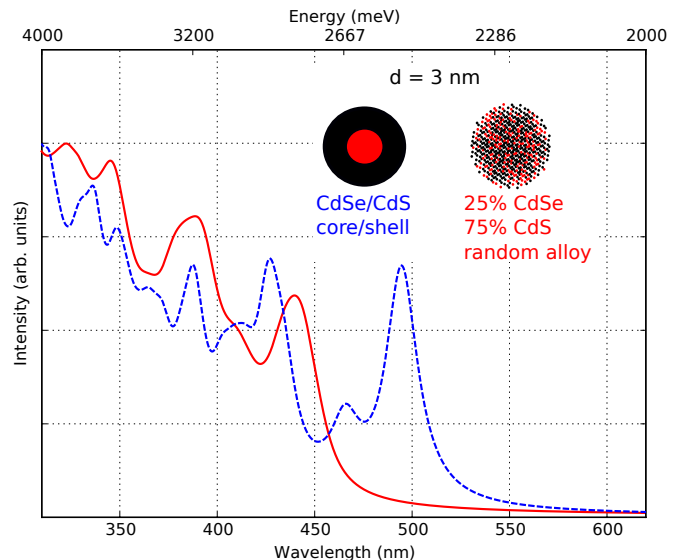


Figure 2. Absorption spectra for $\text{CdSe}_{0.25}\text{S}_{0.75}$ randomly alloyed QDs (solid red) and their CdSe/CdS core/shell counterpart (dashed blue).

mon maximum value, as the quantitative discussion of relative peak heights is beyond the scope of the present work. Instead, we will focus on the energy/wavelength dependence of selected features, in particular the phase dependent spectral position of the energetically lowest absorption peak.

B. Results for type-I Cd(Se,S) and CdSe/CdS QDs

$\text{CdSe}_{0.25}\text{S}_{0.75}$ vs. CdSe/CdS. The absorption spectra for the $\text{CdSe}_{0.25}\text{S}_{0.75}$ randomly alloyed QDs and their CdSe/CdS core/shell counterpart can be found in Fig. 2. As depicted in Fig. 3, the energetically lowest absorption peak for the alloyed QDs can be found at approximately 2.82 eV (440 nm). This is in very good agreement with the experimental UV-Vis value of 2.88 eV (431 nm) as obtained from the nonlinear bowing parameter for the system under consideration.⁴ Also, the randomly alloyed QDs show a small shoulder on the red (smaller energy) side of the second main transition peak that can experimentally and theoretically be attributed to an optically active alloying-induced impurity band and vanishes for larger Se contents.⁴ As additional benchmark for the accuracy of our approach, we use the calculated excitonic gaps for pure CdSe and CdS (absorption curves not depicted here) which are obtained as 2.32 eV (534 nm) and 3.14 eV (395 nm), respectively. This is in good agreement (deviation < 0.1 eV) with experimental results from several studies.^{4,26} Upon phase segregation into the core/shell case, we predict a redshift of approximately -310 meV ($+55$ nm) for the energetically lowest transition. Also, the calculated core/shell spectrum clearly shows—accompanied by a smaller second

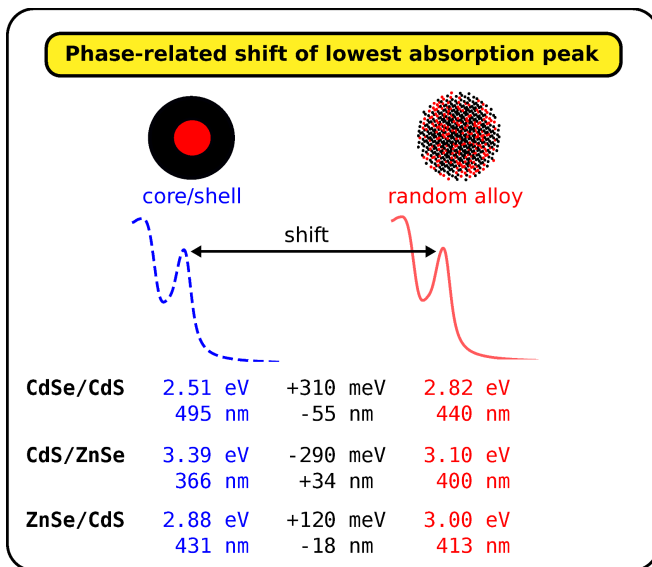


Figure 3. Phase-related difference of the energetically lowest absorption peaks for all systems under consideration.

local maximum—a drop in the absorption intensity on the blue side of the first main transition. Because of the limited number of distinct realizations and the omission of effects like size disorder, phonon-couplings and temperature-induced broadenings, all the smaller peak variations will not be relevant for the comparison with an experimental UV-Vis spectrum, which is usually of a much “smoother” shape. Nevertheless, we think that this feature might be so prominent that it can also be found in an experimental absorption spectrum for the phase-separated CdSe/CdS system under consideration.

C. Results for type-II (Zn,Cd)(Se,S), ZnSe/CdS and CdS/ZnSe QDs

The absorption spectra for the $\text{Cd}_{0.25}\text{Zn}_{0.75}\text{S}_{0.25}\text{Se}_{0.75}$ randomly alloyed QDs and their CdS/ZnSe core/shell counterpart, as well as for $\text{Cd}_{0.75}\text{Zn}_{0.25}\text{S}_{0.75}\text{Se}_{0.25}$ randomly alloyed QDs and ZnSe/CdS core/shell can be found in Figs. 4a and 4b, respectively.

$\text{Cd}_{0.25}\text{Zn}_{0.75}\text{S}_{0.25}\text{Se}_{0.75}$ vs. CdS/ZnSe. We will start with a discussion of the former system, of which the spectrum is depicted in Fig. 4a. In contrast to the type-I Cd(Se,S) system (where the lines were redshifted after phase separation), we now find for the lowest alloy absorption peak at ca. 3.10 eV a blueshift of 290 meV (34 nm) upon separation into the CdS/ZnSe core/shell system (see also Fig. 3). Furthermore, the core/shell spectrum exhibits a different shape with an emphasized intensity minimum between a prominent first and second main absorption band, while the alloy spectrum has very little structure (a quasi-continuous absorption onset) on the blue high-energy/low wavelength side of the main absorption band. According to our simulations, both effects

(blueshift and second main absorption band) should be prominent enough to also be identifiable in a real experimental UV-Vis setup.

$\text{Cd}_{0.75}\text{Zn}_{0.25}\text{S}_{0.75}\text{Se}_{0.25}$ vs. ZnSe/CdS. We will close with a discussion of the counterpart of the preceding type-II system. The absorption spectrum for $\text{Cd}_{0.75}\text{Zn}_{0.25}\text{S}_{0.75}\text{Se}_{0.25}$ randomly alloyed QDs and ZnSe/CdS core/shell is depicted in Fig. 4b. While in the preceding two cases, the random alloy and core/shell cases showed clearly different features, this is much less the case now. The lowest alloy absorption peak at ca. 3.00 eV (see again Fig. 3) now shows a relatively small redshift of 120 meV (18 nm) upon phase separation. Also, the overall shape of the spectrum is slightly different, albeit both show local minima that are separated by the more or less constant small redshift. Nevertheless, the differences are so small that corresponding predictions will presumably exceed the range of validity of our models, and would most likely not be identifiable in real UV-Vis spectra due to the already discussed additional effects and uncertainties. Still, the general trend that we find here might be useful in further studies on this colloidal QD system.

D. Further discussion

It should be emphasized that the energetic shifts observed here are not of the same nature as the commonly observed redshifts in many type-II structures that are induced upon shell growth.^{35,36} The latter shifts can, e.g., result from a reduction of the effective band gap, a change in the work function or, additionally, be strain-induced. Still, they always refer to the bare core system with smaller diameter, while our reference systems are random alloys of the same overall QD size. A random alloy QD often exhibits a much smaller gap than the linearly averaged (“virtual crystal”) gaps of the constituents due to the considerably large nonlinear bowing coefficient.^{4,18} Depending on the materials and sizes under consideration, the redshift that results from an admixture of small band gap material can be larger than shifts upon shell growth and/or size variations. However, the corresponding analysis is beyond the scope of this paper and will be part of future work.

A further analysis in analogy to Ref. 4, (which is not repeated here for the sake of brevity) of the wave functions and oscillator strengths for the here examined core/shell systems shows that the wave functions significantly leak across the barrier over the whole QD and, e.g., in ZnSe/CdS the electron ground state (which is “CdS shell-like”) has considerable overlap with the lowest hole states (“ZnSe core-like”) and is optically active. Therefore, and as already mentioned in Sec. III A, for such small cores and thin shells, the bulk-derived designation as type-II or quasi-type-II is here of limited explanatory power for the QD optical properties. Also, we stress that our non self-consistent method also has inher-

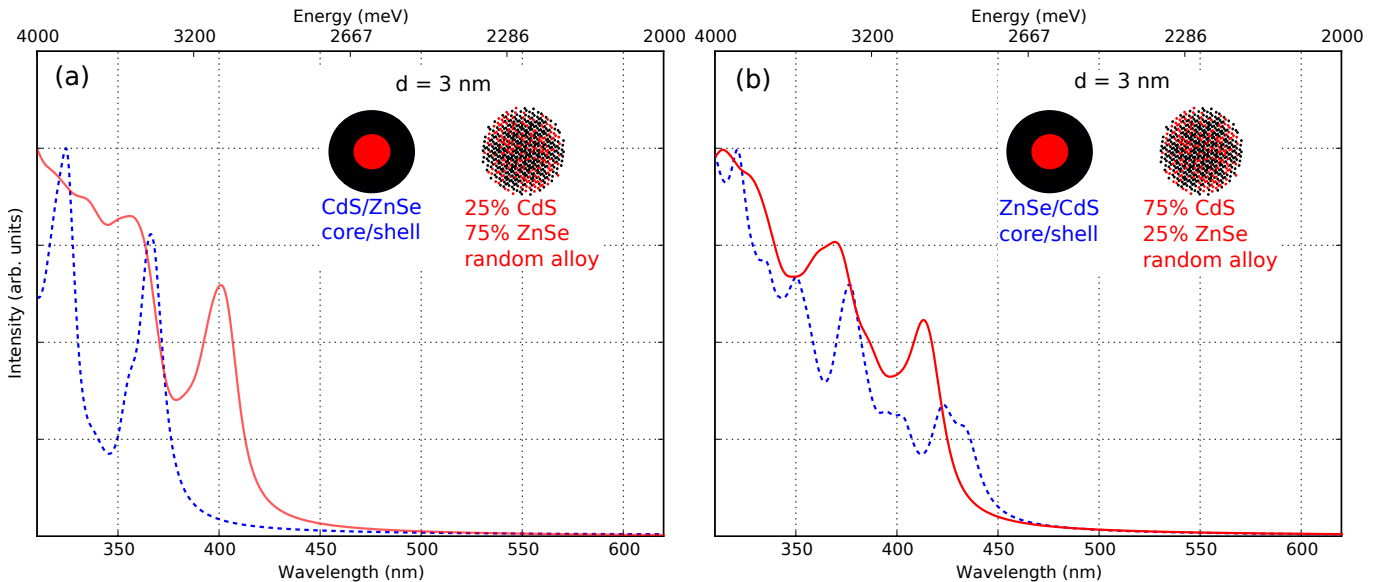


Figure 4. Calculated absorption spectra for (a) $\text{Cd}_{0.25}\text{Zn}_{0.75}\text{S}_{0.25}\text{Se}_{0.75}$ randomly alloyed QDs (solid red) and the CdS/ZnSe core/shell counterpart (dashed blue) and (b) $\text{Cd}_{0.75}\text{Zn}_{0.25}\text{S}_{0.75}\text{Se}_{0.25}$ randomly alloyed QDs (solid red) and their ZnSe/CdS core/shell counterpart (dashed blue).

ent limitations when applied to very small systems. Still, it should be pointed out that it is always more accurate than a corresponding multiband effective mass/ $\mathbf{k} \cdot \mathbf{p}$ calculation, as the latter can analytically be proven to be a limit case of our TB model.⁵

IV. SUMMARY

In randomly alloyed monodisperse semiconductor quantum dots, the relative composition of the constituents is a powerful means to continuously tune the absorption and emission wavelength and further technologically relevant optoelectronic properties. However, the distinction between real solid-solution like alloy QDs and phase-separated core/shell QDs—which are technologically useful on their own, but undesired in some cases—is difficult and usually requires a combination of rather sophisticated tools for structural characterization.

In this paper, which represents a considerable extension of more specialized previous works,^{4,18} we have shown that the optical absorption spectrum of small (3 nm diameter) QDs can in principle be used to differentiate a random alloy phase from a stoichiometrically equivalent core/shell phase. Our model calculations are based on conceptually simple tight-binding calculation, are exact in the substitutional disorder degree of freedom and inhibit local alloy effects like wave function distortions and their microscopical impact on dipole selection rules, as well as nonlinear shifts in the electron and hole quasi-particle spectra.

Our comprehensive scheme only uses bulk band structure properties without additional free parameters and has been applied to calculate the random alloy

vs. core/shell absorption spectrum of one type-I QD system, (i) $\text{CdSe}_{0.25}\text{S}_{0.75}$ vs. CdSe/CdS, and two similar type-II QD systems, (ii) $\text{Cd}_{0.25}\text{Zn}_{0.75}\text{S}_{0.25}\text{Se}_{0.75}$ vs. CdS/ZnSe and (iii) $\text{Cd}_{0.75}\text{Zn}_{0.25}\text{S}_{0.75}\text{Se}_{0.25}$ vs. ZnSe/CdS. In particular, we have analysed the energetic shift of the lowest absorption peak upon phase change and the overall shape of the low energy/large wavelength part of the spectrum. For cases (i) and (ii) we find strong signatures upon core/shell desegregation that should also be identifiable in realistic experimental setups. For case (iii), we also find quantifiable fingerprints, but think that they might be too weak when compared to the overall accuracy of our method.

To give an outlook, we think that the method employed here can be a valuable tool to circumvent more sophisticated structural analysis method for a multitude of further systems. In the future, it can be applied to further colloidal QD systems, as well as larger diameters. When additional disorder degrees of freedom, e.g., size and shape disorder are applied (as long as the computational effort allows to do so), we expect even more accurate predictions.

ACKNOWLEDGMENTS

The author would first and foremost like to thank Z. Hens, but also A. Guille, T. Aubert and E. Brainis for the fruitful collaboration and stimulating discussions that lead to this work. Furthermore, the author would like to acknowledge G. Czycholl, R. Binder and N.-H. Kwong for interesting discussions about the intricacies of the light-matter coupling, is indebted to T. Wehling for the opportunity to carry out this research as part of his group and

thanks M. Schüler and J. Jackson for helpful comments on the manuscript. Also, grants of the North-German Supercomputing Alliance HLRN for computation time and support from the Deutsche Forschungsgemeinschaft, Project No. CZ 31/20-1, “Many-body theory of optical properties for semiconductor nanostructures based on atomistic tight-binding models” are thankfully acknowledged.

Appendix A: Dielectric mismatch effects in core/shell and alloyed quantum dots

Influence of dielectric mismatch. In aqueous solutions ε_{out} will be one order of magnitude larger than ε_{in} . As Σ_{pol} is predominantly a function of $\varepsilon_{\text{out}}^{-1} - \varepsilon_{\text{in}}^{-1}$,²¹ the magnitude of the surface-induced polarization will then be dominated by QD-specific variations of $\varepsilon_{\text{in}}^{-1}$. Whether or not a properly defined E^{coul} will then be subject to the same cancellation effect is a rather involved question (and cannot be answered without a self-consistent approach), but of minor importance for our present paper: All three binary semiconductor materials CdS, CdSe and ZnSe would lead to a more or less identical site-averaged screening coefficient $\varepsilon_{\text{in}}^{-1} \approx 0.2(2)$ (see Refs. 4 and 18 and references therein^{37,38}) for a pure binary QD of the here examined size. Therefore, any randomly alloyed or core-shell separated QD can approximately be characterized by the same value $\varepsilon_{\text{in}}^{-1}$, which results in an identical Σ_{pol} for a given diameter.

Moreover, Σ_{pol} and E^{coul} can still be expected to approximately cancel for a given microstate, geometry and composition, as—in the simplest first order approximation—both stem from a site average weighted with the same probability density $|\psi(\mathbf{r})|^2$.²¹ Within a multiband effective-mass based approach, it has been shown in Ref. 39 that the experimentally accessible excitonic gap is only weakly dependent on the magnitude of the dielectric mismatch at the boundary.

Transferability to alloy and core/shell systems. Due to the above discussed almost constant $\varepsilon_{\text{in}}^{-1}$ for all materials under consideration, we assume the influence of image charge contributions at the core/shell interface to be negligible.⁴⁰ To see whether the cancellation assumption is still valid when comparing the alloyed and core/shell realizations, we performed test calculations of density-density like Coulomb MEs⁴¹

$$V_{ijji}^{\text{ehhe}} = \langle \psi_i^e | \langle \psi_j^h | V_{\text{Coul}} | \psi_j^h \rangle | \psi_i^e \rangle, \quad (\text{A1})$$

where V_{Coul} is the Coulomb operator, for several electron and hole states and randomly selected single alloy microstates, alongside the core/shell QDs. These MEs constitute the largest part of the the quasi-electron quasi-hole attraction. Overall, the discrepancy in the screened Coulomb MEs between the randomly alloyed and corresponding core/shell QDs is roughly between 0.02 eV ($\text{Zn}_{0.75}\text{Cd}_{0.25}\text{Se}_{0.75}\text{S}_{0.25}$ vs equivalent CdS/ZnSe core/shell) and 0.05 eV ($\text{CdSe}_{0.25}\text{S}_{0.75}$ vs equivalent

CdSe/CdS core/shell), while we estimate the absolute accuracy of the absorption spectrum calculated in an empirical TB method to 0.1 eV (at most) in this size regime.

Transferability to higher transitions. Although the results from Refs. 20, 21, and 39 were only obtained for the energetically lowest transitions of unalloyed systems, we found the basic conclusions also to be approximately valid for a large part of the spectrum of bound states of disordered systems in the energetic vicinity of the excitonic gap (see the discussion in Ref. 4). This can presumably be traced back to the fact that we use an empirical TB model that does not only reliably fit the Brillouin zone center, but the dispersion over the whole irreducible wedge for the optically relevant bands,^{5,42} which corresponds to $\delta\Sigma_{\text{bulk}} \approx 0$ over the whole first Brillouin zone. While *GW* calculations practically yield wavevector independent self-energy corrections to the conduction bands for most semiconductors like Si and GaAs,⁴³ the proper modeling can be more complicated for the strongly ionic II-VI compounds examined here for a multitude of reasons.^{44,45} Within our empirical TB model, we are not dependent on the validity of any of those assumptions and their impact on the calculation of higher transitions in II-VI quantum dots and—if available—can also incorporate any additional corrections based on experimental findings. On the other hand, the here employed rather artificial assumption of perfect surface passivation will have a larger impact on higher excited states, so we expect our model to be less accurate when the absorption energies approach the experimentally known ionization continuum.

Impact of disorder effects to Coulomb matrix elements. As already discussed in Refs. 4 and 18, the most prominent consequences of the additional disorder degree of freedom are (i) the resulting large scattering of the single-particle energy levels and (ii) the presence of additional dipole transitions upon the alloy-induced wave function distortion. The disorder-related scattering of the Coulomb MEs takes place on a scale of tens of meV for the sizes under consideration (see Fig. 6 of Ref. 18) and is thus of minor importance for the discussion of the visible spectrum on a corresponding energy scale.

REFERENCES

- ¹Z. Deng, H. Yan, and Y. Liu, *J. Am. Chem. Soc.* **131**, 17744 (2009).
- ²T. Aubert, M. Cirillo, S. Flamee, R. Van Deun, H. Lange, C. Thomsen, and Z. Hens, *Chem. Mater.* **25**, 2388 (2013).
- ³N. Tschirner, H. Lange, A. Schliwa, A. Biermann, C. Thomsen, K. Lambert, R. Gomes, and Z. Hens, *Chem. Mater.* **24**, 311 (2011).
- ⁴D. Mourad, A. Guille, T. Aubert, E. Brainis, and Z. Hens, *Chem. Mater.* **26**, 6852 (2014).
- ⁵J. P. Loehr, *Phys. Rev. B* **50**, 5429 (1994).
- ⁶S. Adachi, *Handbook on Physical Properties of Semiconductors, Volume 3: II-VI Compound Semiconductors* (Springer-Verlag, Berlin/Heidelberg, 2004).
- ⁷R. Blachnik, J. Chu, R. Galazka, J. Geurts, J. Gutowski, B. Hönerlage, D. Hofmann, J. Kossut, R. Levy, P. Michler,

- U. Neukirch, T. Story, D. Strauch, and A. Waag, *Numerical Data and Functional Relationships in Science and Technology / Zahlenwerte und Funktionen aus Naturwissenschaften und Technik. New Series - ... / BD 41 / Part b / Part a*, 1st ed., edited by U. Rössler (Springer-Verlag Berlin and Heidelberg GmbH & Co. K, 1999).
- ⁸Y. D. Kim, M. V. Klein, S. F. Ren, Y. C. Chang, H. Luo, N. Samarth, and J. K. Furdyna, *Phys. Rev. B* **49**, 7262 (1994).
- ⁹H. W. Hölscher, A. Nöthe, and C. Uihlein, *Phys. Rev. B* **31**, 2379 (1985).
- ¹⁰W. Mönch, *J. Appl. Phys.* **80**, 5076 (1996).
- ¹¹P. Han and G. Bester, *Phys. Rev. B* **92**, 125438 (2015).
- ¹²B. Gu, N. H. Kwong, and R. Binder, *Phys. Rev. B* **87**, 125301 (2013).
- ¹³D. J. Chadi, *Phys. Rev. B* **16**, 790 (1977).
- ¹⁴J. Zak, *Physics Letters A* **83**, 287 (1981).
- ¹⁵T. B. Boykin and P. Vogl, *Phys. Rev. B* **65**, 035202 (2001).
- ¹⁶W. Sheng, S.-J. Cheng, and P. Hawrylak, *Phys. Rev. B* **71**, 035316 (2005).
- ¹⁷S. Schulz, D. Mourad, and G. Czycholl, *Phys. Rev. B* **80**, 165405 (2009).
- ¹⁸D. Mourad and G. Czycholl, *Eur. Phys. J. B* **78**, 497 (2010).
- ¹⁹L. J. Sham and T. M. Rice, *Phys. Rev.* **144**, 708 (1966).
- ²⁰C. Delerue, M. Lannoo, and G. Allan, *Phys. Rev. Lett.* **84**, 2457 (2000).
- ²¹M. Lannoo, C. Delerue, and G. Allan, *Phys. Rev. Lett.* **74**, 3415 (1995).
- ²²J. D. Jackson, *Classical Electrodynamics*, 3rd ed. (John Wiley & Sons, New York, 1998).
- ²³C. Delerue, M. Lannoo, and G. Allan, *Phys. Rev. B* **68**, 115411 (2003).
- ²⁴C. d. M. Donegà, *Chem Soc Rev* **40**, 1512 (2011).
- ²⁵O. Chen, J. Zhao, V. P. Chauhan, J. Cui, C. Wong, D. K. Harris, H. Wei, H.-S. Han, D. Fukumura, R. K. Jain, and M. G. Bawendi, *Nat Mater* **12**, 445 (2013).
- ²⁶W. K. Bae, L. A. Padilha, Y.-S. Park, H. McDaniel, I. Robel, J. M. Pietryga, and V. I. Klimov, *ACS Nano* **7**, 3411 (2013).
- ²⁷Some of the forthcoming references deal with wurtzite quantum dots, while we assume a zincblende structure. Similar to the structural analysis in Ref. 3, the conclusions of the present work will presumably also hold for wurtzite and zincblende/wurtzite polytype QDs because of the very similar band gaps in the hexagonal phase.
- ²⁸X. Peng, M. C. Schlamp, A. V. Kadavanich, and A. P. Alivisatos, *J. Am. Chem. Soc.* **119**, 7019 (1997).
- ²⁹L. A. Swafford, L. A. Weigand, M. J. Bowers, J. R. McBride, J. L. Rapaport, T. L. Watt, S. K. Dixit, L. C. Feldman, and S. J. Rosenthal, *J. Am. Chem. Soc.* **128**, 12299 (2006).
- ³⁰J. Ouyang, M. Vincent, D. Kingston, P. Descours, T. Boivineau, M. B. Zaman, X. Wu, and K. Yu, *J. Phys. Chem. C* **113**, 5193 (2009).
- ³¹S. Brovelli, R. D. Schaller, S. A. Crooker, F. Garca-Santamara, Y. Chen, R. Viswanatha, J. A. Hollingsworth, H. Htoon, and V. I. Klimov, *Nat Commun* **2**, 280 (2011).
- ³²S. A. Ivanov, A. Piryatinski, J. Nanda, S. Tretiak, K. R. Zavadil, W. O. Wallace, D. Werder, and V. I. Klimov, *J. Am. Chem. Soc.* **129**, 11708 (2007).
- ³³Z. Ning, H. Tian, C. Yuan, Y. Fu, H. Qin, L. Sun, and H. gren, *Chem. Commun.* **47**, 1536 (2011).
- ³⁴K. Boldt, K. N. Schwarz, N. Kirkwood, T. A. Smith, and P. Mulvaney, *J. Phys. Chem. C* **118**, 13276 (2014).
- ³⁵A. M. Smith and S. Nie, *Acc Chem Res* **43**, 190 (2010).
- ³⁶C. M. Tyrakowski, A. Shamirian, C. E. Rowland, H. Shen, A. Das, R. D. Schaller, and P. T. Snee, *Chem. Mater.* **27**, 7276 (2015).
- ³⁷D. R. Penn, *Phys. Rev.* **128**, 2093 (1962).
- ³⁸A. Franceschetti, H. Fu, L. W. Wang, and A. Zunger, *Phys. Rev. B* **60**, 1819 (1999).
- ³⁹V. A. Fonoberov, E. P. Pokatilov, and A. A. Balandin, *Phys. Rev. B* **66**, 085310 (2002).
- ⁴⁰A quantitative assessment of this assumption is beyond the scope of our present model.
- ⁴¹Behold that this nomenclature refers to the electron-hole picture,⁴⁶ while in the electron-electron picture these MEs come from an exchange-like self-energy variation.
- ⁴²O. Marquardt, D. Mourad, S. Schulz, T. Hickel, G. Czycholl, and J. Neugebauer, *Phys. Rev. B* **78**, 235302 (2008).
- ⁴³R. W. Godby, M. Schlüter, and L. J. Sham, *Phys. Rev. B* **37**, 10159 (1988).
- ⁴⁴O. Zakharov, A. Rubio, X. Blase, M. L. Cohen, and S. G. Louie, *Phys. Rev. B* **50**, 10780 (1994).
- ⁴⁵M. Rohlfing, P. Krüger, and J. Pollmann, *Phys. Rev. Lett.* **75**, 3489 (1995).
- ⁴⁶G. Onida, L. Reining, and A. Rubio, *Rev. Mod. Phys.* **74**, 601 (2002).